Korean J. Chem. Eng., 36(2), 255-264 (2019)
DOI: 10.1007/s11814-018-0188-4

pISSN: 0256-1115
eISSN: 1975-7220

A hydrophilic-oleophobic chitosan/SiO_2 composite membrane to enhance oil fouling resistance in membrane distillation

Fatemeh Ardeshiri[*,], Ahmad Akbari[**,***], Majid Peyravi[*,†], and Mohsen Jahanshahi[*]**

*Nanotechnology Institute, Babol Noshirvani University of Technology, Shariati Ave., Babol, 47148-71167, Iran
**Institute of Nanoscience and Nanotechnology, University of Kashan, P. O. Box: 87317-53153, Kashan, Iran
***Department of Carpet, Faculty of Architecture & Art, University of Kashan, Kashan, Iran
(*Received 18 June 2018 • accepted 14 November 2018*)

Abstract−To develop an inexpensive and simple technology and increase anti-oil fouling resistance for membrane distillation applications, a hydrophilic/oleophobic nanocomposite membrane was fabricated by using SiO_2/Chitosan (CT) sol solution coating with different volume ratios (0.5 : 1, 1 : 1 and 2 : 1 v/v) on PVDF membrane surface. The formation of SiO_2/CT layer on membrane surface was confirmed by Fourier transform infrared (FTIR) spectroscopy and energy-dispersive X-ray spectroscopy (EDX). The influence of hydrophilic nanocomposite layer on the characteristics of membranes, including in-air water contact angle, morphology, porosity, liquid entry pressure of water (LEPw) and direct contact membrane distillation (DCMD) performance, was investigated. The results show that the composite membrane (SiO_2/CT (1 : 1 v/v)- PVDF membrane) by adding of 0.5 and 1 g/L gasoline concentrations not only incurred fouling but also a higher flux with respect to the neat membrane in each gasoline concentration. During 8 hours continuous desalination process of saline gasoline emulsion solution (20 gr/L NaCl solution containing 0.5 gr/L gasoline), it was found that all modified membranes had high performance stability in comparison with the neat membrane, the modified membrane showed high performance stability and flux without decreased salt rejection (99.9%). At the end, we conducted performance comparison between the prepared membranes in current work and presser based process.

Keywords: Hydrophilic-oleophobic Nanocomposite, SiO_2/CT Sol Solution, Anti-oil Fouling Resistance, DCMD Performance

INTRODUCTION

Regarding water scarcity for drinking and producing it from seawater/brackish water resources, various membrane technologies have been developed for water distillation. Membrane desalination (MD) has been known as a relatively new separation technique to provide fresh water from saline water resources [1]. MD is a separation technology based on the partial vapor pressure gradient between the hot feed solution and cold distillate stream that is usually used to desalinate hypersaline solution such as briny shale oil produced water and seawater [2,3]. MD process, due to low operating temperature, low hydrostatic pressure and eventually low energy consumption using waste heat and renewable energy sources, is considered a useful method to distill saline water. Since the MD process only allows the water vapor passing through membrane pores, as a result it can theoretically have 100% rejection for non-volatile solute [4-6].

According to mentioned advantages, the membrane should have both high hydrophobicity and liquid entry pressure (LEP) that can prevent the penetration of aqueous solution inside the membrane pores, which is known as wetting phenomenon, and consequently results in reducing MD performance [7,8].

Commercial hydrophobic polymeric membranes such as poly vinylidene fluoride (PVDF), polytetrafluoroethylene, and polypropylene have been widely used in this process [9]. Conventional hydrophobic membranes can only desalinate saline water without foulant. When they are applied to desalinate saline water containing hydrophobic components (e.g., oil and organic foulants), fouling occurs due to the strong hydrophobic - hydrophobic interaction [10,11]. Foulants possibly attach on the hydrophobic membrane surface leading to blocking the membrane pores, fouling and thereby decreasing water vapor flux. Following this assumption, developing composite MD membrane with a hydrophobic substrate and an underwater superoleophobic top surface is the key requirement to increase oil-fouling resistance of PVDF membrane for MD applications. The hydrophilic/oleophobic surfaces are typically in-air hydrophilic and underwater oleophobic, which prevents oil adhesion on the surface. In general, if coating, in addition to having hydrophilicity property, is underwater oleophobic, it can create a strong interaction between the water and hydrophilic surface via hydrogen bonds that leads to forming a hydration layer. The hydration layer acts as a robust barrier in the attachment of hydrophobic foulant on the surface [12-14].

In recent years, many studies have been made on separation of oil-water emulsion by coating hydrophilic/oleophobic material on stainless steel mesh and PVDF membranes. Li et al. [15] synthesized superhydrophilic and superoleophobic ZnO-based coated mesh for separation of oil and water with high yield. Zhang et al. [16] prepared a self-cleaning underwater superoleophobic mesh by the layer-by-layer assembly of sodium silicate and TiO_2 nanoparti-

†To whom correspondence should be addressed.
E-mail: majidpeyravi@nit.ac.ir, majidpeyravi@gmail.com
Copyright by The Korean Institute of Chemical Engineers.

cles on the stainless steel mesh for emulsion. However, the following reports are based on the use of hydrophilic/oleophobic coating on hydrophobic membrane to distill hypersaline brine from shale gas/oil produced water in order to reduce fouling by hydrophobic compounds. Hou and coworkers [17] prepared a novel dual-layer composite membrane with underwater-superoleophobic/hydrophobic asymmetric wettability using poly (vinyl alcohol)/silica nanoparticles hybrid fibrous coating for robust oil-fouling resistance in membrane distillation desalination. In another study, this group coated polytetrafluoroethylene substrate with a nanocomposite fibrous network comprising cellulose acetate and silica nanoparticles for robust oil-fouling resistance in MD [18].

Chitosan (CT) is widely applied in preparing membranes as coating layer since it has good film forming ability, biocompatibility, nontoxicity and antibacterial activity. Also, the presence of amine groups makes it a cationic polyelectrolyte that can cause a strong electrostatic interaction with PVDF membrane and Polyethersulfone membrane [19,20]. On the other hand, because of active sites existence, amino (NH2) and hydroxyl (OH) group on the backbone of chitosan structure can absorb some metal through covalent bonding and form stable nanocomposite [21,22]. Many researchers used CT and its composite on PVDF membrane for oil/water separation [23-25]. Regarding high performance of CT in oil/water separation, some researchers used it for MD applications. Chanachai et al. [26] used chitosan-coated hydrophobic PVDF hollow fiber membrane to treat oily feed for protection against wetting. Wang and co-workers [27] prepared a composite membrane with a hydrophobic substrate and a superhydrophilic skin layer (CT/fluorosurfactant complexes/SiO_2 nanocomposite) to investigate oil-water emulsion treatment with and without surfactant using direct contact membrane distillation (DCMD) process.

In this study, we have successfully coated a hydrophilic/oleophobic layer on PVDF membrane via a facile route and investigated antifouling performance of composite membrane using DCMD. The chemical structure, morphology, roughness and contact angle of neat and modified membranes were determined. The membrane fouling was comprehensively evaluated by the change of the gasoline (as a foulant) and saline concentrations. Additionally, we conducted separation of gasoline in water emulsion using pressure based process and eventually compared its performance with MD process.

MATERIALS AND METHODS

1. Materials

To prepare MD membranes, polyvinylidene fluoride polymer (PVDF, MW=530,000 gr mol^{-1}, Koreha Company) as the membrane substrates and N, N-dimethylformamide (DMF, >99.8%, Merck) as the solvent were used. Materials used for modification of the membrane surface included glutaaldehyde (GA), chitosan (CT, medium molecular weight), tetraethyl orthosilicate (TEOS), ammonia (30%), ethanol (99.8%) and acetic acid, which were supplied from Merck. The MD membrane performance was examined by sodium chloride (NaCl, >99%, Dr. Mojallali) solution. Distilled water was used throughout this study.

2. Preparation of PVDF Membrane

The developed membranes were prepared by phase inversion method [28]. In brief, the casting solution was composed of PVDF and DMF, while the casting solution concentration was kept at 16%. For preparing the casting solution, a certain amount of PVDF powder was gradually added to DMF and mixed using magnetic stirrer for 15 h at 25 °C. Then the dope solution was degassed at room temperature for about 3 h to release the trapped air bubbles. The mixed solutions were cast using a doctor blade with a thickness of 100 μm on the polyester non-woven fabric. Then, this was smoothly immersed in non-solvent bath (water) at 30 °C after being exposed 30 s in air. The flat membranes were stored in water for at least 1 day to remove the excess DMF solvent. Ultimately, the membranes were dried between two filter papers for 24 h at room temperature before used.

3. Preparation of SiO_2/CT Nanocomposite Membrane

The SiO_2/CT sole-gel nanocomposite was prepared according to the previous studies with a little change [29]. First, 1 g CT was completely dissolved in 1 L of 2% (v/v) acetic acid under stirring for 24 h at 25 °C. Then, the SiO_2 sol solution was prepared by Stober method using the following procedures: a solution of 50 ml distilled water, 8 ml ammonia, 5 ml TEOS and 250 ml ethanol was added to round-bottom glass flask added to the solution and then stirred simultaneously overnight at 25 °C.

In the following, a milky suspension of CT/SiO_2 formed immediately by adding SiO_2 sol solution into CT solution with 0.5 : 1, 1 : 1 and 2 : 1 ratios (v/v). Then, 0.5 ml of GA solution (as cross linker) was added to each of suspension solutions under stirring for 12 h.

Afterwards, membranes were coated by immersing the membrane surface into the SiO_2/CT nanocomposite solutions for 3 min at 25 °C and the dried at 70 °C for 30 min. Finally, the membranes were rinsed with distilled water.

4. Membrane Characterization

Attenuated total reflection of prepared flat-sheet membranes was investigated using an FT-IR spectrometer (model WQF-520, Germany). The IR spectra were recorded in a wave number range of 450-4,350 cm^{-1} by cumulating 32 scans at a signal resolution of 4 cm^{-1}.

Field emission scanning electron microscope (FESEM, Model: Mira 3-XMU) was used to examine the surface morphology of membranes. Before SEM analysis, all samples were coated with thin gold layer. The images are obtained in accelerating voltage 15 KV under vacuum conditions. Energy-dispersive X-ray (EDX) spectroscopy is an analytical method applied to determine the chemical characterization of the prepared membranes. Contact angle measurements (CA, Model: 500M, Iran) were used to determine water contact angle in water. The measurements were carried out for each sample at three random locations to minimize the experimental error, and then a reliable value was presented. Nevertheless, because of the capillary effects on contact angle measurement, it cannot be used to determine the hydrophilicity of membrane surfaces alone. Therefore, to estimate the surface hydrophilicity of membranes, the free surface energy ($-\Delta G_{SL}$) was calculated by following formula, using obtained contact angle [31,32]:

$$-\Delta G_{SL} = \gamma_L\left(1+\frac{\cos\theta}{\Delta}\right) \quad (1)$$

where γ_L is the surface tension of the liquid (γ_L=72.8 mJ/m^2 for pure water at 25 °C), θ is the average contact angle and Δ is actual surface area divided by the planar area. The planar area was determined from atomic force microscopy (AFM, model: Easyscan2 flex) and actual surface area was 10 μm×10 μm. Also, AFM was used to study the surface morphology and roughness. The membrane surface images were obtained in the mentioned scan area, and the average surface roughness parameters was employed to examine the morphology of the prepared membranes.

4-1. Membrane Wettability

LEPw measurement was done to examine the membrane wettability. LEPw is the minimum value of hydrostatic pressure which the feed liquid penetrates into the membrane pores [30]. According to the procedure presented by Smolder and Franken [31], LEPw measurement was conducted using a dead-end filtration cell at room temperature. The pure and composite membranes were placed in a horizontal steel cell which consisted of two upper and down parts. The up-cell was filled with distilled water and was connected to nitrogen gas. First, the pressure of up-cell was kept at the constant pressure (about 0.25 bar) at least for 10 minutes. Then, the pressure was gradually increased in small steps (0.25 bar) during the measurement. When the first permeate drop was obtained, the corresponding pressure was recorded as the LEPw value.

4-2. Membrane Porosity

The gravimetric measurement is used to determine the membrane porosity. The membranes with size 1 cm×1 cm were immersed in ethanol for 30 min. After mopping with tissue paper, their weights were measured as wet weight (m_2). The porosity (ε) of the prepared membranes was obtained using Eq. (2) [32]:

$$\varepsilon = \frac{(m_2 - m_1)\rho_1}{\rho_1 m_2 + (\rho_2 - \rho_1)m_1} \quad (2)$$

where m_1 is the weight of the dry membrane (the membranes placed in an oven at 60 °C for 24 h before immersing in ethanol), m_2 is the weight of the wet membrane, ρ_1 and ρ_2 are the density of PVDF (1.78 gr/cm^3) and ethanol (0.789 gr/cm^3), respectively.

5. Preparation of Gasoline Feed Solution

The feed solution was a gasoline in water emulsion prepared by mixing gasoline and NaCl salt through stirring at 15,000 rpm for 30 min. In this work, the effects of gasoline (0.5 and 1 g/L) and salt (10-30 g/L) on permeate flux of membranes were investigated.

6. Experimental Procedure

DCMD experiments (one of common configurations of MD) were performed to evaluate the flux and rejection of the developed membranes. The membrane plate modules with 30.4 cm^2 effective area consisted of two chambers including hot feed and distillate. The circulation of feed and distillate in the membrane module was carried out using two magnetic pumps (MP-215R, china). The hot feed was saline gasoline emulsion, the temperature and flow rate were 68 °C and 400 ml/min, respectively. The distilled water employed in permeate was kept constant at 22 °C by the ice bath. Also, the flow rate of permeate was adjusted at 200 ml/min. The flow rate was measured by rotameter. The mass of permeate of MD membranes was measured using an electronic balance placed at the side of the distillate tank. The water flux was calculated using Eq. (3):

$$\text{Flux} = \frac{M}{A \times t} \quad (3)$$

Flux (Kg/m^2 h) is described as amount of permeated water M (Kg) per unit area of effective membrane A (m^2) per unit operation time t (h). Also, the rejection ratio was calculated according to the following formula:

$$\text{Rejection}\ (\%) = \left(1 - \frac{C_P}{C_F}\right) \times 100 \quad (4)$$

Here C_P and C_F correspond with concentrations of permeate and feed solutions, respectively. Salt concentrations of aqueous NaCl solutions were determined via a conductivity meter (Model: WA-2017SD, Taiwan).

The experiments of flux recovery ratio, FRR, were conducted to evaluate the antifouling properties of the membrane. At first, the water flux was determined (J_{w1}), and after desalination of 20 gr/L salt solution containing 500 mg/L gasoline for 3 h, and then the water flux of membranes was measured after water rinsing, J_{w2}. FRR was calculated by the following expression:

$$\text{FRR}\ (\%) = \frac{J_{w2}}{J_{w1}} \times 100 \quad (5)$$

To compare filtration and MD process, filtration experiments were carried with 0.5 gr/L gasoline in water emulsion. Gasoline concentrations were determined with a UV-Vis absorption spectroscopy (Shimadzu UV-3100, Japan).

RESULTS AND DISCUSSION

1. SiO_2/CT-PVDF Membrane

The developed membranes in this study were fabricated by coating SiO_2/CT nanocomposite on the PVDF membrane surface. As previously mentioned, CT is a natural polysaccharide that has in-

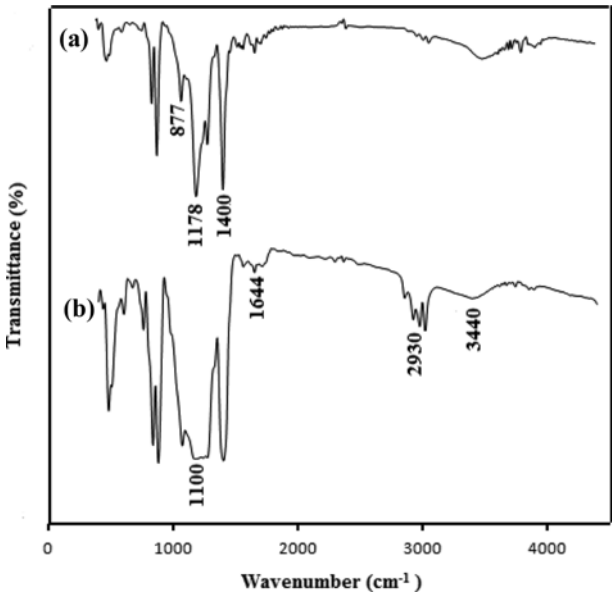

Fig. 1. ATR-IR spectra of (a) PVDF membrane (b) SiO_2/CT (1 : 1)-PVDF membrane.

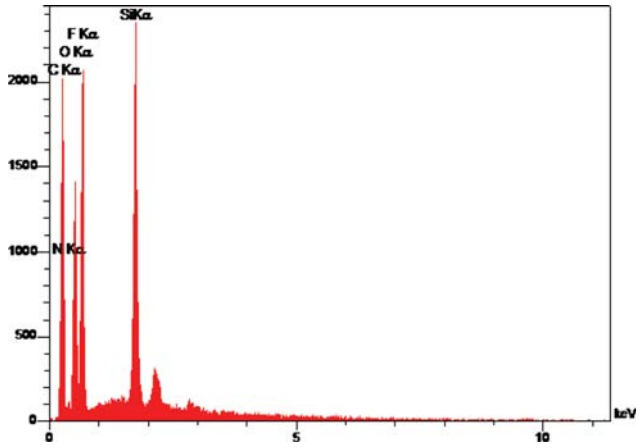

Fig. 2. EDX analysis of SiO_2/CT (1 : 1 v/v)-PVDF membrane.

teresting properties such as non-toxicity, low cost and high hydrophilicity. These properties make CT an effective material for water treatment and oil/water separation. On the other hand, nanoscale SiO_2 as one of the multifunctional inorganic nanoparticles has been widely applied in the membrane modification process. As reported by Huang et al. [33], the surface roughness and thus the hydration area of PVDF microfiltration membrane was enhanced by coating of nano SiO_2 particle on membrane surface. They found that the hydration force of the modified PVDF membrane increased

Table 1. The percentage composition of different elements of SiO_2/CT (1 : 1 v/v)-PVDF membrane

Membrane	C	O	F	Si	N
Modified membrane	38	24	24	77	15

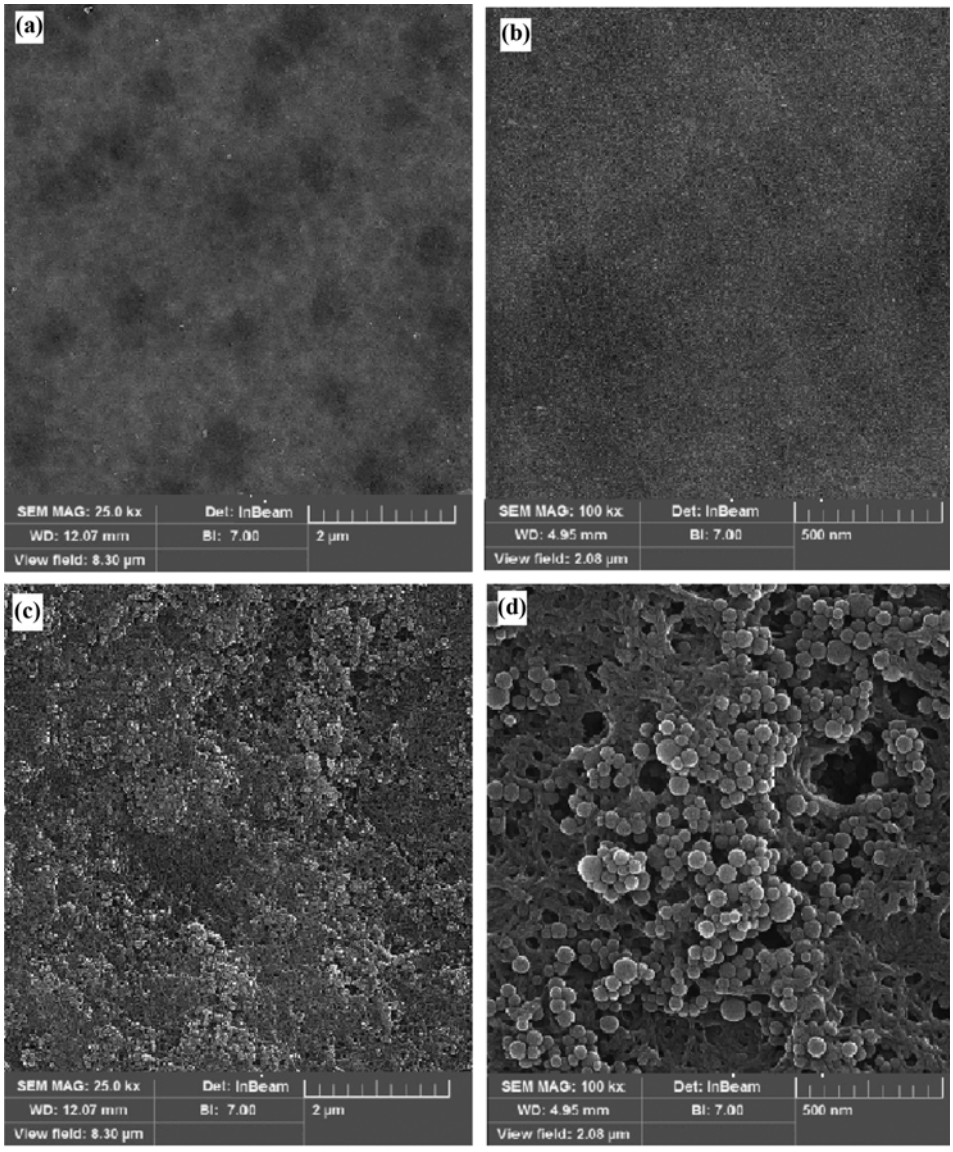

Fig. 3. The SEM images of membrane surfaces: The neat PVDF membrane ((a), (b)) and the modified membrane with SiO_2/CT (1 : 1 v/v) nanocomposite ((c), (d)).

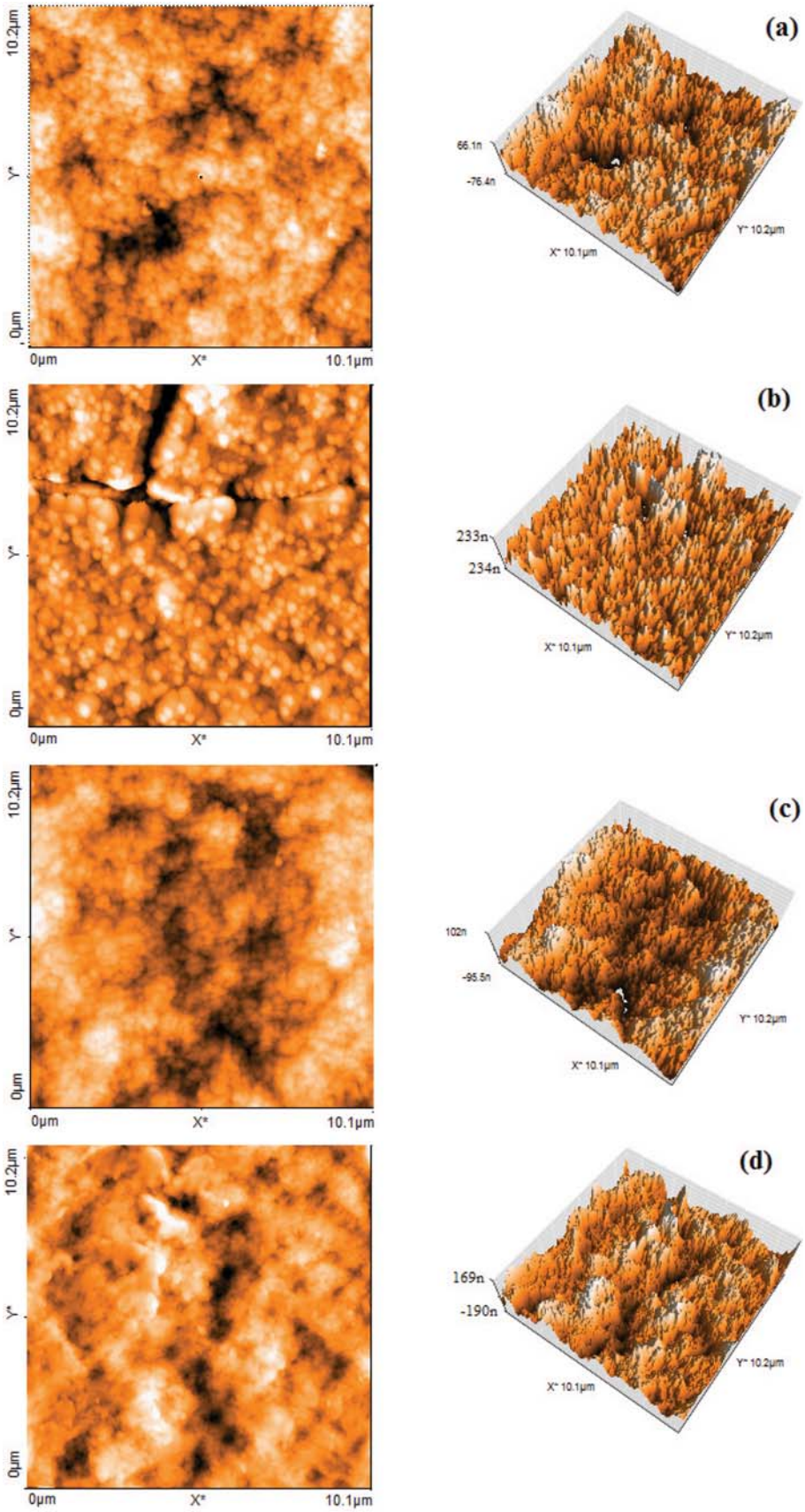

Fig. 4. Two- and three-dimensional surface AFM images of PVDF membranes prepared with (a) pure PVDF membrane (b) SiO_2/CT-PVDF (0.5 : 1 v/v) membrane (c) SiO_2/CT-PVDF (1 : 1 v/v) membrane (d) SiO_2/CT-PVDF (2 : 1 v/v) membrane.

considerably and presented the surface underwater superoleophobic, which were known as vital properties for robust anti-oil-fouling MD. Wang et al. [34] used SiO_2 nanoparticles for fabricating oleophobic nanocomposite membrane for direct contact membrane distillation due to increase the surface roughness and creating hierarchical morphology that are essential for hydrophilic/underwater oleophobic surfaces. In the present study, SiO_2 nanoparticles were used as a high reactive nanoparticle due to presence of hydroxyl functional on SiO_2 surface, which makes it a suitable candidate for hydrophilic modification by CT polymer. Therefore, during the preparation of SiO_2/CT nanocomposite by sol-gel method, the silanol groups resulting from hydrolysis of TEOS reacted with the hydroxyl functional groups of CT polymer. The GA used as cross linker function can create imine bonding through reaction between its aldehyde groups with amine groups of CT polymer [35,36].

FTIR spectra of neat and modified PVDF membranes are illustrated in Fig. 1. It can be observed that the peaks at 1,400, 1,178, 877 cm^{-1} are attributed to the C-H, C-F and C-C stretching vibration bonds, respectively (Fig. 1(a)) [37]. In Fig. 1(b), the peaks at 2,930, 2,870 cm^{-1} belong to the CH_2 and CH_3 stretching vibration of GA; and the broad vibration band at 3,440 cm^{-1} corresponds to the amine (NH_2) and hydroxyl (OH) stretching of CT polymer. The peak located at 1,100 cm^{-1} can be assigned to the stretching bond of Si-O. The bond at 1,644 cm^{-1} validates the existence of imine groups (C=N) [38-40]. All observed data confirmed CT/SiO_2 nanocomposite has been attached on the PVDF membrane surface.

The EDX was further applied to confirm the formation of SiO_2 in SiO_2/CT nanocomposite on the PVDF membrane surface. The EDX spectra result and compositions of different elements of modified membrane are shown in Fig. 2 and summarized in Table 1, respectively. The existence of Si, N, C and O elements in nanocomposite PVDF membrane was detected by the strong peaks in EDX.

2. Morphological Study

The surface morphology of the PVDF membranes prepared with and without the SiO_2/CT (1 : 1 v/v) nanocomposite was investigated using FE-SEM, and the obtained images are presented in Fig. 3. A comparison between images shows that the SiO_2 nanoparticles randomly distributed on membrane surface even though some nanoparticles oriented to form aggregates induced by the van der Waals interparticle or interparticle termination [41]. On the other hand, the modified membrane has rough surface originating by SiO_2 nanoparticles. The surface roughness is usually more desired for MD process because it provides higher free surface energy, and hence, more strong resistance against wetting [42]. On the other hand, it is completely clear that CT thin layer coated the overall membrane surface, which leads to the surface of modified membrane to be dense.

The two- and three-dimensional surface AFM images of the pure and modified PVDF membranes with different ratios of SiO_2/CT nanocomposite at scan size of 10 μm×10 μm can be observed in Fig. 4. From Fig. 4(a), from the ridge and valley structure visually seen in surface of pure PVDF membrane the surface seems to be smooth. However, the ridges were not pungent in case of pure membrane. As can be seen in Figs. 4(b) to (d), by incorporation of SiO_2/CT nanocomposite onto the PVDF membrane surface, the surface roughness suddenly increases and the ridge-valley structure appears sharper as compared with the pure PVDF membrane.

Table 2. Surface roughness parameters of pure and modified PVDF membranes

Membrane	Roughness		
	S_a	S_q	S_z
Pure PVDF	20.71	26.13	195.57
SiO_2/CT (0.5 : 1) PVDF	44.64	57.21	327.16
SiO_2/CT (1 : 1) PVDF	32.73	39.59	246
SiO_2/CT (2 : 1) PVDF	37.47	49.52	291.61

The surface roughness parameters of the membranes are summarized in Table 2. The roughness parameters are expressed in terms of the mean roughness (S_a), the root mean square of the Z data (S_q) and the mean difference between the highest peaks and lowest valleys (S_z) that were calculated by SPM DME software. Table 2 shows the modified PVDF membranes with a SiO_2/CT top layer with different volume ratios had higher roughness values as compared to the pure PVDF membrane. The increment of surface roughness can be attributed to presence SiO_2 nanoparticles in the top layer of composite membranes. However, the roughness is not much significant in comparison with the pure PVDF membrane that can be attributed to non-uniform distribution of the SiO_2 nanoparticles on surface. Anyhow, AFM data show that the presence of SiO_2/CT with different ratios on surface affected the surface roughness and also increased surface area. Note that, regarding increasing of surface roughness (R_a), contact of surface area with vapor molecular increased. Accompanied with enhanced roughness and surface area, mass transfer resistance decreased, thereby the vapor permeate rate accelerated through micro-pores membrane [43-46].

3. Structural Assay of SiO_2/CT-PVDF Membrane

The in-air water contact angle results were determined by sessile drop method that was consistent with the results of surface roughness. Table 3 illustrates the water contact angle for the prepared membranes. The in-air water contact angle of the pure membrane was 80°. This indicates that PVDF membrane was hydrophobic in air. After coating layer on PVDF surface with volume ratios of SiO_2/CT sol, the in-air water contact angles were reduced, which indicated the modified membranes were in-air hydrophilic. As shown in Table 3, the free energy surface of PVDF membranes increased after coating CT/SiO_2. The presence of hydrophilic functional groups such as hydroxyl and amine on membrane surface, results showed higher the free energy surface and hydrophilicity as compared with pure PVDF membrane. Based on the reviewed literature, by increasing hydrophilicity, interaction between surface and vapor molecules improved showing that effective role on MD

Table 3. The contact angle and the free energy surface for neat and composite membrane

Membranes	Contact angle (°)	$(-\Delta G_{SL})$ (mJ/m^2)
Pure PVDF	80	85.56
SiO_2/CT (0.5 : 1) PVDF	67.25	100.59
SiO_2/CT (1 : 1) PVDF	63.44	105.56
SiO_2/CT (2 : 1) PVDF	68.62	98.99

Table 4. The mean values of the porosity and LEP of the PVDF membranes with and without the SiO_2/CT nanocomposite

Membranes	Porosity (%)	Thickness (μm)	LEP (bar)
Pure PVDF	53	180	6-7
SiO_2/CT (0.5 : 1)-PVDF	41	280	5.6
SiO_2/CT (1 : 1)-PVDF	53	277	5
SiO_2/CT (2 : 1)-PVDF	41.6	287	5.8

membrane performance [47-49].

LEPw is a significant characterization because it evaluates wetting resistance of membranes. The LEPw value should be as high as possible to overcome water penetration through membrane pores. The high LEPw value can be obtained through two routes: by an increment in surface hydrophobicity or a reduction in pore size [50].

Thickness and porosity of pure and modified PVDF membranes are compared in Table 3. As reflected from Table 3, the thickness of modified membranes is higher than pure PVDF membrane due to the SiO_2/CT coating layer. The porosity values of the PVDF composite membranes were lower than pure PVDF membrane or similar with one. The porosity reduction of SiO_2/CT (0.5 : 1) - PVDF and SiO_2/CT (2 : 1) - PVDF can be, respectively, attributed to high concentrations of CT and SiO_2. The low porosity enhanced mass transfer resistance, thereby the water vapor permeance rates slowed during MD process [51].

As seen in Table 4, the composite membranes had lower LEPw values (about 5 bar) compared to the neat PVDF membrane (6-7 bar). Regarding the deposition of hydrophilic CT/SiO_2 nanocomposite in the entrance of the pores and membrane thicker, therefore, it is rational that the LEP value decreased partially after hydrophilic/oleophobic coating. However, the loss of LEP was not very impressive in comparison with the pure PVDF membrane. (ii) Since the membrane structures and bulk pores were unchanged after surface modification by hydrophilic/oleophobic layer, the loss of LEP was not considerable [52]. However, the difference in LEPw values of the neat and composite membranes was not very impressive, which can be attributed to cross-linker effects. The cross-linking CT polymer chains by GA, because of the inorganic network, decreased the mobility of polymer chains (free volume) and the space resulted in compact and integration structure on surface, which can be prevented from further reduction of LEP [53,54].

4. Membrane Performance

Fig. 5 shows the obtained results of the flat sheet membranes during 8 h of operation times. It was found that all these four membranes showed uncertain flux permeate, while salt rejection of all of them was about 99.99% during DCMD process. In this case, the DCMD experiments were carried out by using 20 gr/L NaCl salt solution containing 500 mg/L gasoline; the temperatures of hot feed and cold permeate were kept constant at 68 °C and 22 °C, respectively. During the first 2 h of MD process, the permeate flux of pure PVDF membrane decreased very fast. When operation time was more than 2 h, a stable flux was observed. In fact, for the unmodified membrane more fouled surface occurred in a relatively short time. This predictable result is attributed to hydrophobic properties of PVDF membrane. It is accepted, when hydrophobic

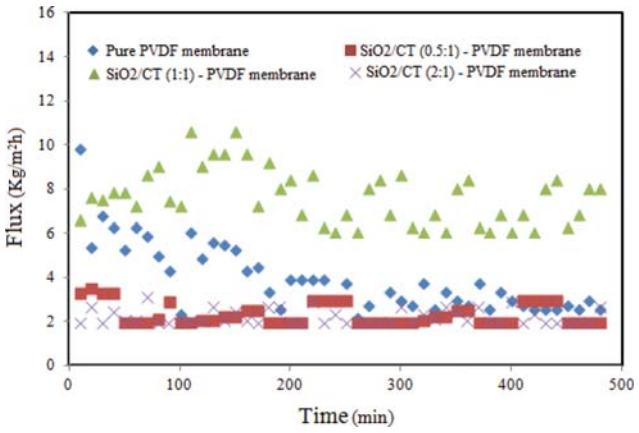

Fig. 5. Variation of flux along with operating time.

membrane with lower surface free energy is applied for the treatment of water-containing oil compounds, due to hydrophobic-hydrophobic interaction, the oil compounds easily will accumulate on the membrane surface. This case leads to form a precipitation layer and increases risk of pores blocking [10,11]. The blocking of pores is a great problem for MD application because it creates an additional resistance on the surface and slows the vapor transfer rate from the hot side to cold side, thereby a considerable reduction in flux occurs.

In comparison, the PVDF membrane with different volume ratios of SiO_2/CT top layer during DCMD experiments indicated stable performance toward that pure PVDF membrane. Therefore, the modified membranes, unlike neat membrane being able to pass vapor molecules through micro-pores except oil compound is mainly due to the formation of hydration force near surface [55]. As can be observed in Fig. 5, the permeate flux of SiO_2/CT (1 : 1 v/v)-PVDF quite stabilized about 9.01-6 kg/m^2h, which was highest flux among membranes. While, the SiO_2/CT (0.5 : 1 v/v)-PVDF membrane and SiO_2/CT (2 : 1)-PVDF membrane have constant flux about 1.96-3.3 kg/m^2h. The obtained lower flux can be attributed to results of high thickness and low porosity. However, all composite membranes were resistant to fouling due to the presence of hydrophilic layer that led to a hydration layer. The hydration layer formation near the surface was associated with increased surface energy as a rational reason for confirming high performance of the SiO_2/CT composite membrane. As a conceptual mechanism, the hydration layer was caused by strong hydrogen bonding between water molecular and unreacted hydroxyl and amine groups of surface resulted to create a physical and energetic barrier to avoid the adsorption of oil compounds on the surface [56]. Accordingly, the formation of this layer increased the evaporation rate and facilitated the vapor penetration though the micropores of the SiO_2/CT composite membranes. The in-air WCA values of prepared membranes after long-term DCMD performance are presented in Table 5. The results indicate that only a slight decrease in the in-air WCA of modified membranes occurred, which means that the membranes yet preserve hydrophilic/oleophobic properties. These results in this study were consistent with the obtained in-air WCA values after long-term DCMD process in previous researches [57].

Table 5. The in-air WCA of prepared membranes after DCMD performance

Sample	Pure PVDF	SiO_2/CT (0.5 : 1)-PVDF membrane	SiO_2/CT (1 : 1)-PVDF membrane	SiO_2/CT (2 : 1)-PVDF membrane
The in-air WCA after DCMD	60.52	46.80	51.49	52.34

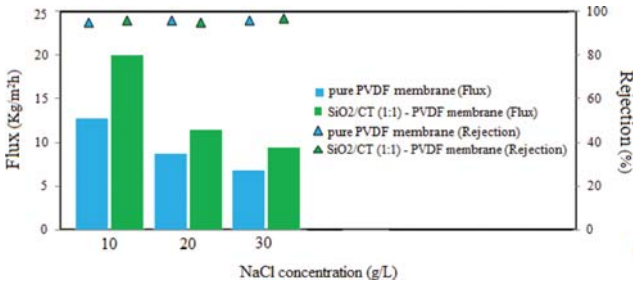

Fig. 6. Effect of NaCl concentration on the DCMD performance of different membranes.

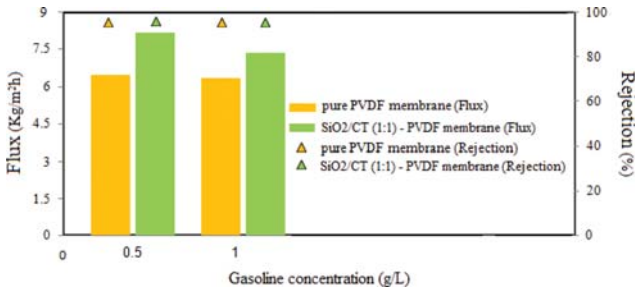

Fig. 7. Effect of gasoline concentration on the DCMD performance of different membranes, the NaCl concentration was 20 gr/L.

5. Effect of Salt Concentration on the DCMD Performance

The effect of different concentrations of NaCl aqueous solutions (10-30 g/L) containing 500 mg/L gasoline on the flux and salt rejection of the neat and modified membranes (SiO_2/CT (1 : 1 v/v) - PVDF membrane) is illustrated in Fig. 6. As expected, for each membrane, the 10 gr/L NaCl solution showed more permeate flux compared with other NaCl concentrations. It can be found that with increasing of salt concentration from 10 gr/L to 30 g/L, a reduction trend of the permeate flux occurred for all membranes, even though this trend was more considerable for the modified membrane. On the basis of previous studies, the reduction of flux with the salt concentration increase can be ascribed to the decreased vapor pressure (driving force) of salt solution at higher concentration, which is induced from the reduction of water activity. Moreover, the formation of additional boundary layer on membrane surface, namely polarization effects, can be considered as another reason [58,59].

It is pertinent to mention that the significant permeate flux reduction of the composite membrane compared with the origin membrane was probably attributed to modification of membrane surface, which led to an increase in membrane thickness that was induced by cross-linker effects, as already mentioned. Consequently, the high thickness prevented vapor molecules transfer though membrane pores, and hence increased the mass transfer resistance on hot feed side [60,61].

6. Effect of Oil Concentration on the DCMD Performance

Fig. 7 shows the DCMD permeate fluxes and salt rejection of the prepared membranes at constant concentration of salt solution (20 gr/L) with different gasoline concentrations (0.5 and 1 gr/L). By increasing gasoline concentration in 20 gr/L salt solutions, the flux of PVDF membrane was decreased from 6.4 to 6.28 kg/m^2h, while it was reduced from 8.50 to 7.43 kg/m^2h for the modified membrane. It shows that (i) the flux behavior of all corresponding membranes has a decreasing trend when the gasoline concentration was increased from 0.5 gr/L to 1 gr/L in salt solutions and also, (ii) fouling has seriously occurred for neat membrane. Additionally, the permeate flux of PVDF nanocomposite membrane when used for desalination of 1 gr/L gasoline emulsion is only slightly lower than that of 0.5 gr/L gasoline emulsion distilled by the same membrane. It suggests that the flux decline of the modified membrane was negligible by increasing the foulant concentration in the feed. This observation is attributed to higher efficiency of PVDF surface modification.

7. Fouling Investigation of MD Membrane

The most effective parameter on the MD membrane performance, especially in DCMD configuration, is FRR. Fig. 8 shows the comparison in the normalized flux before cleaning and FRR of

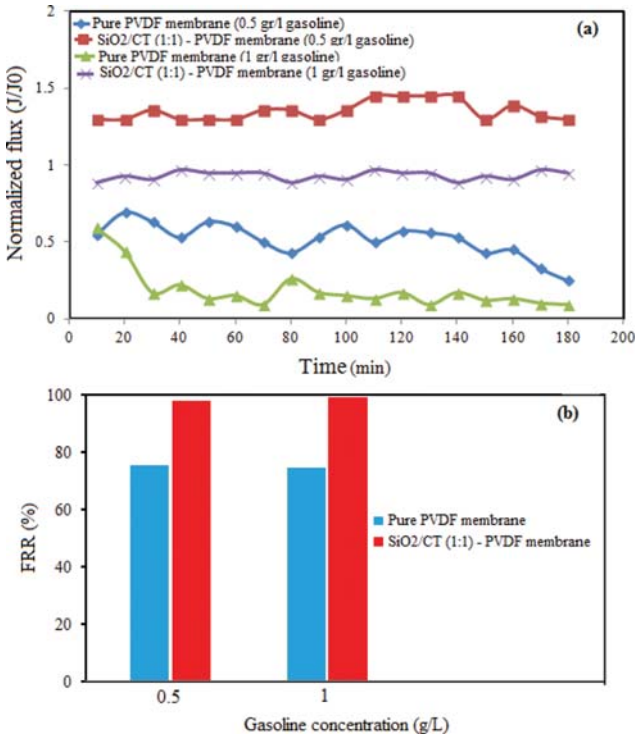

Fig. 8. (a) The DCMD performance before cleaning (b) FRR of the prepared membranes.

the neat and modified membranes conducted by the 20 gr/L salt solution containing two different concentrations of gasoline (0.5 and 1 g/L). As seen in Fig. 8(a), significant fouling was observed for the pure PVDF membrane in DCMD experiments before cleaning by an admirable decline of the normalized flux in a relatively short time. In comparison, the composite membrane had a constant normalized flux during DCMD performance before cleaning. FRR of the nanocomposite membrane reached 98% and it is approximately 25% higher than that of the neat membrane. From the results, the hydrophilic coating of SiO_2/CT nanocomposite on surface of the PVDF membrane effectively decreased the foulant tendency for deposition on the membrane surface, which indicates an achievement in anti-oil fouling properties of the modified membrane.

Generally, hydrophilic/oleophobic membrane (SiO_2/CT (1 : 1)-PVDF) has been applied for oil/water emulsion separation under based-pressure process. In this regard, oil/water emulsion separation was conducted by both MD and regular filtration processes. The emulsion was prepared from 0.5 gr gasoline in 1 L distilled water. As shown in Fig. 9 under MD process, the flux of the pure membrane significantly reduced with increasing operation time, while the flux of the SiO_2/CT composite membrane (1 : 1 v/v) showed a constant trend which was higher than the pure membrane.

Under based-pressure process (Fig. 10), a constant flux of 0.9-1.15 kg/m^2h was obtained for the neat PVDF membrane, which was the lowest flux among the evaluated membranes for both processes. This might be viewed as the result of lower porosity, high LEP and hydrophobicity properties. We expected that for the nanocomposite membrane in 5 bar pressure, the oil compound penetrates though membrane pores and decreases rejection. But, the flux of composite membrane for over 5 h was higher than the neat membrane, about 10.52-13.78 kg/m^2h, without the rejection reduction occurring (about 96%). This trend corresponds with the MD test results but with this difference that rejection was 99.99%.

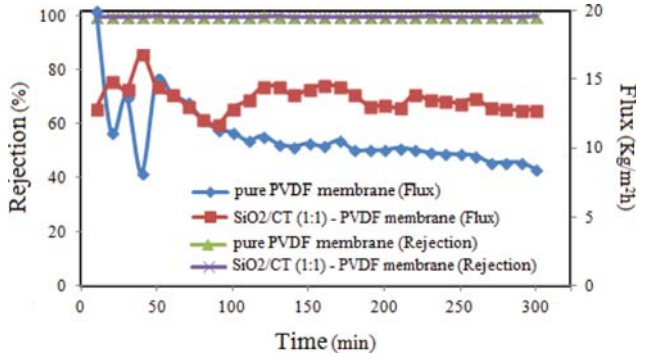

Fig. 9. The DCMD performance of the prepared membrane for 0.5 gr/L gasoline in water emulsion.

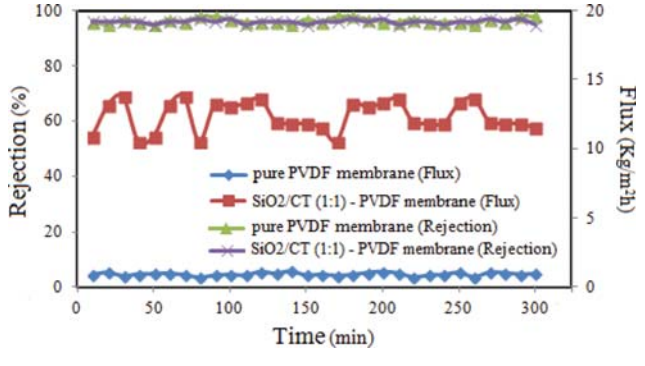

Fig. 10. The filtration performance of the prepared membrane for 0.5 gr/L gasoline in water emulsion.

Based on the obtained results, the DCMD process indicated comparable performance or even better than the based-pressure process for the modified nanocomposite membrane. The obtained flux of the modified membrane had similar trend in both processes, even though the rejection resulting from MD experiments was higher than the filtration tests. Nevertheless, we should not ignore this note that there are important differences between two processes returned to energy consumption, hydrostatic pressure, operating temperature which encouraged us to use MD process for oil/water emulsion separation [4-6].

CONCLUSION

PVDF flat sheet composite membranes were successfully fabricated using one-step coating of SiO_2/CT sol solution with different volume ratios on the surface of the PVDF micro-porous membrane. The effects of SiO_2/CT layer on MD performance and different characterization of membranes were investigated. With the coating of SiO_2/CT, the porosity of membranes decreased in comparison with neat membrane; however, the LEP value slightly decreased from 7 to 5 bar, mainly due to the partial tendency of water molecules to hydrophilic surface. The presence of SiO_2 nanoparticle on composite membranes surface increased roughness, thereby affecting results of contact angle. During DCMD experiment of 20 gr/L salt solution with 500 mg/L gasoline, the flux permeate of modified membrane (SiO_2/CT (1 : 1 v/v) layer) was significantly enhanced by coating of hydrophilic layer, reaching a rejection of above 99%, which was higher compared with the unmodified membrane. It is believed that the developed composite membranes here are promising for this suggestion that hydrophilic/oleophobic membrane can contribute to fouling reduction.

ACKNOWLEDGEMENT

The authors acknowledge the funding support of Babol Noshirvani University of Technology through Grant program No. BNUT/389026/97.

REFERENCES

1. J. Zuo and S. Bonyadi, *J. Membr. Sci.*, **497**, 239 (2016).
2. L. F. Duméea, K. Searsa, J. Schütza, N. Finna and C. Huynha, *J. Membr. Sci.*, **351**, 36 (2010).
3. S. Ragunath, S. Roy and S. Mitra, *Sep. Purif. Technol.*, **170**, 427 (2016).
4. R. Moradi, J. Karimi-Sabet, M. Shariaty-niassar and Y. Amini, *Korean J. Chem. Eng.*, **33**, 2993 (2016).
5. P. Pouresmaeel-Selkjani, M. Jahanshahi and M. Peyravi, *High Per-*

form. Poly., **29**, 1 (2016).
6. M. Yao, Y. Chul Woo, L. D. Tijing, J. S. Choi and H. K. Shon, *Desalination*, **440**, 146 (2018).
7. N. Shafaei, M. Jahanshahi, M. Peyravi and Q. Najafpour, *Korean J. Chem. Eng.*, **33**, 2968 (2016).
8. Z. Wang, Y. Chen, X. Sun, R. Duddua and S. Lin, *J. Membr. Sci.*, **559**, 183 (2018).
9. D. Sun, M. Q. Liu, J. H. Guo, J. Y. Zhang, B. B. Li, D. Y. Li, D. Sun and M. Q. Liu, *Desalination*, **370**, 63 (2015).
10. Y. Woo, Y. Chen and L. D. Tijing, *J. Membr. Sci.*, **529**, 234 (2017).
11. C. Boo, J. Lee and M. Elimelech, *Environ. Sci. Technol.*, **50**, 12275 (2016).
12. A. Jomekian, R. Mosayebi Behbahani, T. Mohammadi and A. Kargar, *Korean J. Chem. Eng.*, **34**, 440 (2017).
13. M. Peyravi, A. Rahimpour and M. Jahanshahi, *J. Membr. Sci.*, **473**, 72 (2015).
14. S. Jo and Y. Kim, *Korean J. Chem. Eng.*, **33**, 3203 (2016).
15. J. Li, L. Yan, W. Li, J. Li, F. Zha and Z. Lei, *Mater. Lett.*, **153**, 62 (2015).
16. L. Zhang and Y. Zhong, *Scient. Repor.*, **3**, 2326 (2013).
17. D. Hou and C. Ding, *Desalination*, **428**, 240 (2018).
18. D. Hou and Z. Wang, *J. Membr. Sci.*, **546**, 179 (2018).
19. K. Ekambaram and M. Doraisamy, *Coll. Surf. A: Phys. Eng.*, **52**, 49 (2017).
20. Y. Cui, M. Meng, D. Sun, Y. Liu, J. Pan, X. Dai and Y. Yan, *Korean J. Chem. Eng.*, **34**, 600 (2017).
21. P. R. Solanki, A. Kaushik, A. A. Ansari, A. T, B. D. Malhotra, *Sens. Actuators, B.*, **137**, 727 (2009).
22. D. E. S. Santos, C. G. T. Neto, J. L. C. Fonseca and M. R. Pereira, *J. Membr. Sci.*, **325**, 362 (2008).
23. Y. Du, *RSC. Adv.*, **7**, 41838 (2017).
24. N. Cao and Q. Lyu, *Chem. Eng. J.*, **326**, (2017).
25. J. Fan and J. Duan, *Water, Air, Soil Pollut.*, **227**, 163 (2016).
26. A. Chanachai and K. Meksup, *Sep. Purif. Technol.*, **72**, 217 (2010).
27. Z. Wang and S. Lin, *Water Res.*, **112**, 38 (2017).
28. F. Esfandian, M. Peyravi, A. A. Qoreyshi, M. Jahanshahi and A. Shokuhi Rad, *Arabi. J. Chem.*, (2017).
29. J. Liu, P. Li, L. Chen, Y. Feng, W. He, X. Yan and X. Lü, *Surf. Coat. Technol.*, **307**, 171 (2016).
30. G. Rácz, S, Kerker, Z. Kovács and G, Vatai, Peri. *Poly. Chem. Eng.*, **58**, 81 (2014).
31. K. Smolder and A. C. M. Franken, *Desalination*, **72**, 249 (1989).
32. M. H. Gu, J. Zhang, X. L. Wang, H. J. Tao and L. T. Ge, *Desalination*, **192**, 160 (2006).
33. Y. X. Huang, Z. Wang, J. Jin and S. Lin, *Environ. Sci. Technol.*, **51**, 13304 (2017).
34. Z. Wang, J. Jin, D. Hou and S. Lin, *J. Membr. Sci.*, **516**, 113 (2016).
35. A. Ghaee, M. Shariaty-Niassar, J. Barzin and T. Matsuura, *Chem. Eng. J.*, **165**, 46 (2010).
36. R. Moradi, J. Karimi-Sabet and M. Shariaty-niassar, *Korean J. Chem. Eng.*, **33**, 2953 (2016).
37. A. Bahgat Radwan, Adel M. A. Mohamed and Aboubakr M. Abdullah, *Surf. Coat. Technol.*, **289**, 136 (2016).
38. T. M. Budnyak, I. V. Pylypchuk, V. A. Tertykh, E. S. Yanovska and D. Kolodynska, *Nano. Resear. Lett.*, **10**, 87 (2015).
39. H. Lu, H. An and Z. Xie, *Int. J. Biol. Macromol.*, **56**, 89 (2013).
40. Y. Shirosaki, *J. Ceram. Soc. Jpn.*, **120**, 555 (2012).
41. L. Ahmadian-Alam, M. Kheirmand and H. Mahdavi, *Chem. Eng. J.*, **284**, 1035 (2016).
42. N. Q. Zhan, Y. X. Li, C. Q. Zhang, Y. Song, H. G. Wang and L. Sun, *J. Colloid Interface Sci.*, **345**, 491 (2010).
43. M. Peyravi, A. Rahimpour and M. Jahanshahi, *J. Membr. Sci.*, **473**, 72 (2015).
44. D. Emadzadeh, W. J. Lau and T. Matsuura, *Chem. Eng. J.*, **237**, 70 (2014).
45. M. Ghanbari, D. Emadzadeh and W. J. Lau, *Desalination*, **377**, 152 (2016).
46. R. R. Darabi, M. Peyravi, M. Jahanshahi and A. A. Q. Amiri, *Korean J. Chem. Eng.*, **34**, 2311 (2017).
47. M. Bhadra, S. Roy and S. Mitra, *Desalination*, **378**, 37 (2016).
48. S. Mansouri, S. Khalili, M. Peyravi, M. Jahanshahi, R. R. Darabi and F. Ardeshiri, *Korean J. Chem. Eng.*, **35**, 2256 (2018).
49. M. Khajouei, M. Peyravi and M. Jahanshahi, *J. Membr. Sci. Res.*, **3**, 2 (2018).
50. L. D. Tijing, Y. Chul Woo, W. G. Shim and T. He, *J. Membr. Sci.*, **502**, 158 (2016).
51. Z. Wang, D. Hou and S. Lin, *Environ. Sci. Technol.*, **50**, 3866 (2016).
52. E. Guillen-Burrieza, M. O. Mavukkandy, M. R. Bilad and H. A. Arafat, *J. Membr. Sci.*, **515**, 163 (2016).
53. Y. H. Su, Y. L. Liu, D. M. Wang, J. Y. Lai, M. D. Guiver and B. Liu, *J. Power Sources*, **194**, 206 (2009).
54. D. S. Kim, H. B. Park, J. W. Rhim and Y. M. Lee, *Sol. Sta. Ioni.*, **176**, 117 (2005).
55. J. Zheng, L. Li and H. K. Tsao, *Biophys J.*, **89**, 158 (2005).
56. A. Babaei Rostam, M. Peyravi, M. Ghorbani and M. Jahanshahi, *Appl. Surf. Sci.*, **427**, 17 (2017).
57. H. J. Wei, T. Y. Tsai and Y. H. Weng, *Korean J. Chem. Eng.*, **33**, 1362 (2016).
58. M. Safavi and T. Mohammadi, *Chem. Eng. J.*, **149**, 191 (2009).
59. A. Rahimpour, M. Jahanshahi and M. Peyravi, *J. Environ. Health Sci. Eng.*, **12**, 55 (2014).
60. S. Majidi Salehi, G. D. Profio, E. Fontananova and F. P. Nicoletta, *J. Membr. Sci.*, **504**, 220 (2015).
61. J. Zhang, Z. Song, B. Li, Q. Wang and S. Wang, *Desalination*, **324**, 1 (2013).